Combined operando studies of new electrode materials for Li-ion batteries

**Jean-Claude Jumas · Moulay Tahar Sougrati ·
Alexis Perea · Laurent Aldon ·
Josette Olivier-Fourcade**

Abstract The performances of Li-ion batteries depend on many factors amongst which the important ones are the electrode materials and their structural and electronic evolution upon cycling. For a better understanding of lithium reactivity mechanism of many materials the combination of X-Ray Powder Diffraction (XRPD) and Transmission Mössbauer Spectroscopy (TMS) providing both structural and electronic information during the electrochemical cycling has been carried out. Thanks to the design of a specific electrochemical cell, derived from a conventional Swagelock cell, such measurements have been realised in *operando* mode. Two examples illustrate the greatness of combining XRPD and TMS for the study of $LiFe_{0.75}Mn_{0.25}PO_4$ as positive electrode and TiSnSb as negative electrode. Different kinds of insertion or conversion reactions have been identified leading to a better optimization and design of performing electrodes.

Keywords *Operando* Mössbauer · Li-ion batteries · Electrochemical cell ·
Insertion reaction · Conversion reaction · Phosphates · Sn-based intermetallics

1 Introduction

The development of high energy and power Li-ion batteries for portable power tools applications, automotive electric transportation (hybrid and electrical vehicles), electrical storage of renewable energies (small and medium size outfits), leads to intensive world-wide research on new electrode materials and electrolytes [1]. The performances of Li-ion batteries depend on many factors amongst which the important ones are the electrode materials and their structural and electronic evolution upon cycling. At present, the performance of the currently used electrode materials

J.-C. Jumas (✉) · M. T. Sougrati · A. Perea · L. Aldon · J. Olivier-Fourcade
Institut Charles Gerhardt (UMR 5253 CNRS), Université Montpellier 2,
CC 1502, Place E. Bataillon, 34095 Montpellier Cedex 5, France
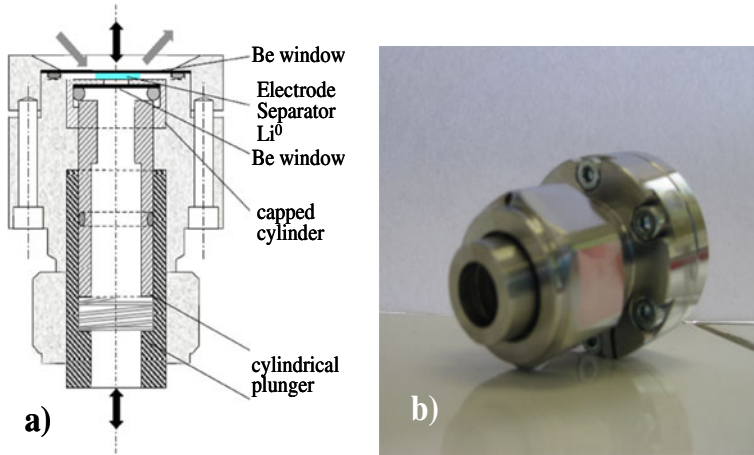e-mail: jumas@univ-montp2.fr

Fig. 1 Electrochemical cell for *operando* measurements: **a** Schema, **b** Photo

(C-based as negative and lithiated transition metal oxides as positive) has reached its upper theoretical limit and new materials are required. The research of new electrode materials of high performance for Li-ion batteries requires a better understanding of the electrochemical reactions that take place during the charge/discharge processes and ageing mechanisms. For this objective the *ex situ* studies of electrode materials are now extensively completed by *in situ* measurements using complementary tools such as X-ray Powder Diffraction (XRPD) and Transmission Mössbauer Spectroscopy (TMS) allowing both structural and electronic characterizations of materials under the conditions of the electrochemical cycling. Concerning TMS, the most recent advances in this kind of measurements were recently reviewed in a special issue of the MERDJ dedicated to its application in the field of batteries [2]. The highest advances of *in situ* measurements are without doubt *operando* techniques, allowing the study of materials during cycling thanks to the development of specific electrochemical cells [3]. It is worth noting that an *in situ* experiment can be qualified "*operando*" only if it is done while the system is operating (during chemical or electrochemical reactions, heating, etc.).

In this paper two examples will be presented to highlight the capabilities of combining *operando* XRPD and TMS in the field of new electrode materials for positive (Fe-based materials) and negative (Sn-based materials) electrodes.

2 Electrochemical cell for operando measurements

A new electrochemical cell specially designed for *operando* experiments at synchrotron facilities both for X-ray Diffraction and X-ray Absorption [3] has been slightly modified to be used also for TMS. Note that all the results shown in this work are obtained by Mössbauer and XRD analyses. Derived from a conventional Swagelock cell (Fig. 1) it allows measurements both in reflection mode (XRPD) or transmission mode (TMS).
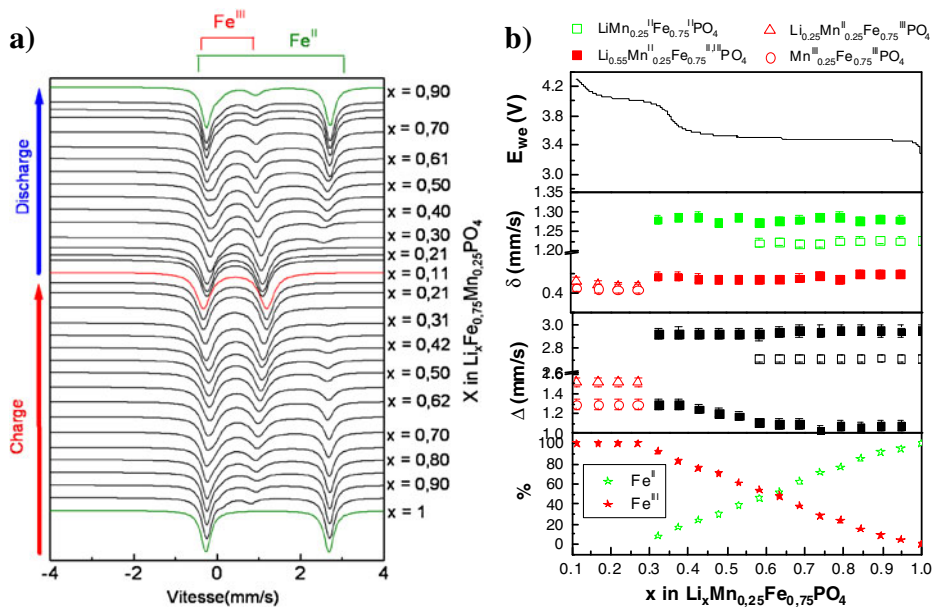
Fig. 2 **a** *operando* ^{57}Fe TMS patterns collected during the charge/discharge of LiMn$_{0.25}$Fe$_{0.75}$PO$_4$/Li cell; **b** evolution of potential, hyperfine parameters and contribution Fe^{II}/Fe^{III} during the 1st charge

3 LiMn$_{0.25}$Fe$_{0.75}$PO$_4$ as positive electrode

Lithium iron phosphate LiFePO$_4$ with an olivine structure has become of great interest as a promising positive electrode for the next generation of Li-ion batteries because of its low cost, safety and environmental compatibility [4]. Many studies have attempted to improve the electrochemical performances of the material and the partially substituted phases LiMn$_y$Fe$_{1-y}$PO$_4$ would introduce the advantage of combining the good electrochemical performances of LiFePO$_4$ with a higher potential for Mn (4.1 V compared with 3.4 V vs Li$^+$/Li for Fe) in order to enhance the energy density. *Operando* XRPD and ^{57}Fe TMS analyses have been used to investigate the evolution of iron local environment, oxidation state and lattice structure during the electrochemical redox process of LiMn$_{0.25}$Fe$_{0.75}$PO$_4$ [5, 6]. The cells were charged and discharged using a C/40 rate (1 Li/40 h), at room temperature in the voltage range 2.75–4.3 V. *Operando* XRPD scan was recorded over 1 h in which Li extraction/insertion was performed and the results correspond to a change of composition of $\Delta x = 0.025$ Li (where x is in Li$_x$Mn$_{0.25}$Fe$_{0.75}$PO$_4$/C) . A 2 h acquisition time was used for the *operando* TMS measurement. Each spectrum corresponds to $\Delta x = 0.05$ extracted/inserted Li.

Figure 2 illustrates the TMS spectra obtained during the first charge for the *operando* measurements and shows the evolution of all Mössbauer hyperfine parameters. Figure 3 depicts the evolution of the *operando* XRPD patterns and the corresponding galvanostatic curves. For clarity reasons, only the main diffraction peaks are represented ($16 \leq 2\theta < 19°$ and $29 \leq 2\theta < 31°$). For $0.95 \leq x < 1$, the TMS spectrum (Fig. 2a) and XRPD pattern (Fig. 3) are similar to those obtained for
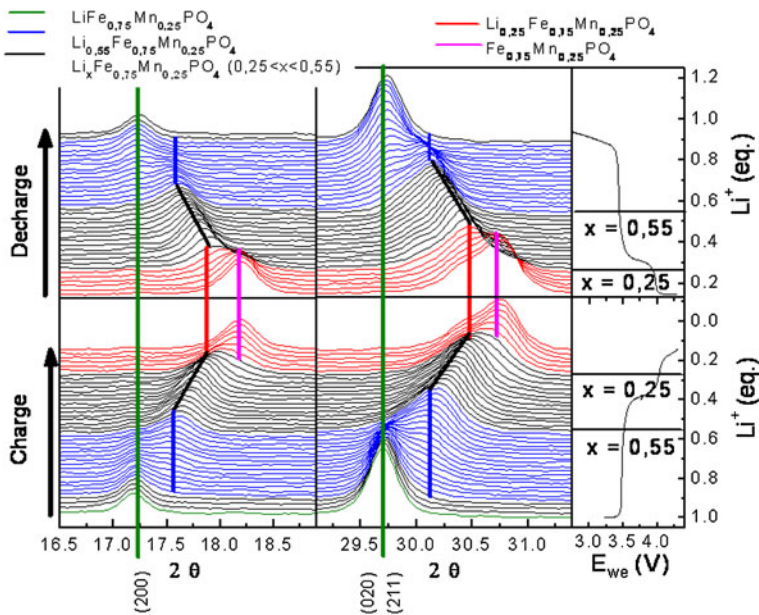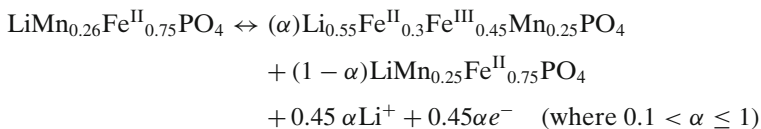
Fig. 3 *Operando* XRPD patterns collected during the charge/discharge of LiMn$_{0.25}$Fe$_{0.75}$PO$_4$/Li cell

the pristine materials. However, significant changes begin to appear in the domain $(0.55 \leq x < 0.95)$ and confirm the coexistence of two phases, the pristine material and a partially delithiated one. At $x = 0.9$, the XRPD pattern shows that new peaks of an olivine-like phase appear. At $x = 0.55$ the (020) peak of the phase LiMn$^{II}_{0.25}$Fe$^{II}_{0.75}$PO$_4$ disappears in the XRPD patterns. From these observations, we propose the coexistence of LiMn$^{II}_{0.25}$Fe$^{II}_{0.75}$PO$_4$ and Li$_{0.55}$Mn$^{II}_{0.25}$Fe$^{II,III}_{0.75}$PO$_4$ during this step. The plateau of the first region corresponds to the Fe^{II}/Fe^{III} redox reaction which is clearly evidenced from the TMS spectra. In addition to the Fe^{II} doublet from the olivine phase, a second doublet appears ($\delta = 0.42$ mms^{-1} and $\Delta = 1.10$ mms^{-1}, Fig. 2b attributed to a Fe^{III} species. At $x = 0.9$, a third doublet was observed ($\delta = 1.28$ mms^{-1} and $\Delta = 2.75$ mms^{-1} (Fig. 2b) and was attributed to a new phase formation. XRPD pattern observation allows us to propose the following composition for this new phase: Li$_{0.55}$Mn$^{II}_{0.25}$Fe$^{II,III}_{0.75}$PO$_4$.

The Mössbauer probe permits us to evaluate the Fe^{II}/Fe^{III} ratio and then the composition of this mixed valence phase as Li$_{0.55}$Fe$^{II}_{0.3}$Fe$^{III}_{0.45}$Mn$_{0.25}$PO$_4$.

For this first region $(0.55 \leq x < 0.95)$ the two-phases mechanism can be written as:

$$LiMn_{0.26}Fe^{II}_{0.75}PO_4 \leftrightarrow (\alpha)Li_{0.55}Fe^{II}_{0.3}Fe^{III}_{0.45}Mn_{0.25}PO_4$$
$$+ (1 - \alpha)LiMn_{0.25}Fe^{II}_{0.75}PO_4$$
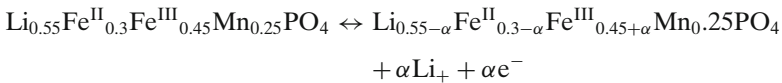$$+ 0.45\,\alpha Li^+ + 0.45\alpha e^- \quad \text{(where } 0.1 < \alpha \leq 1)$$

The second region $(0.25 \leq x \leq 0.55)$ is characterized by a sloppy increase of the potential up to 4.03 V. A systematic shift of the diffraction peak of (020) at $2\theta \sim 29.5°$ of the phase Li$_{0.55}$Fe$^{II}_{0.3}$Fe$^{III}_{0.45}$Mn$_{0.25}$PO$_4$ (Fig. 3) suggests a solid solution occurring

Fig. 4 TMS spectra obtained for $Li_xFe^{III}_{0.75}Mn_{0.25}PO_4 (x \leq 0.25)$
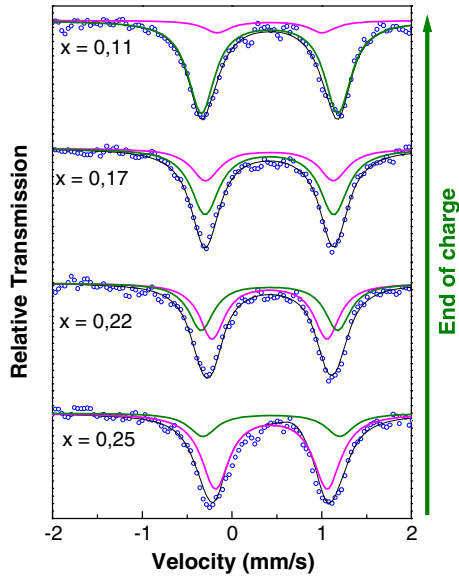
in this domain. In this region, the isomer shift and quadrupole splitting of Fe^{II} as well as the Fe^{III} isomer shift remain unchanged, whereas the quadrupole splitting of Fe^{III} increases gradually with the oxidation of iron indicating a significant lattice change (Fig. 2b), confirming the XRPD results. In fact, Fe^{III} is more sensitive to lattice distortion than Fe^{II} even though the origin of this distortion is due to the second near neighbours. In this domain the one phase mechanism can be described by the following reaction:

$$Li_{0.55}Fe^{II}_{0.3}Fe^{III}_{0.45}Mn_{0.25}PO_4 \leftrightarrow Li_{0.55-\alpha}Fe^{II}_{0.3-\alpha}Fe^{III}_{0.45+\alpha}Mn_0.25PO_4$$
$$+ \alpha Li_+ + \alpha e^-$$

The third region $(0.1 \leq x < 0.25)$ corresponds to the oxidation of Mn^{II} to Mn^{III} which occurs during the short plateau around 4.03 V. The coexistence of the phase $Li_{0.25}Fe^{III}_{0.75}Mn_{0.25}PO_4$ with the totally delithiated phase indicates the occurrence of a two-phases reaction as:

$$Li_{0.25}Fe^{III}_{0.75}Mn_{0.25}PO_4 \leftrightarrow \beta Fe^{III}_{0.75}Mn^{III}_{0.25}PO_4$$
$$+ (1 - \beta)Li_{0.25}Fe^{III}_{0.75}Mn_{0.25}PO_4$$
$$+ 0.25\beta Li^+ + 0.25\beta e^-$$
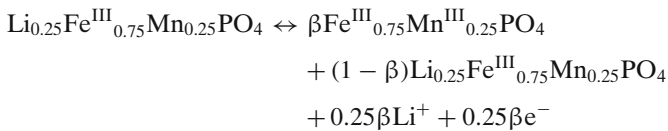
The Fe^{II} has been almost completely oxidized at the beginning of this plateau, but the TMS spectra continues to evolve indicating that the Fe local environment is affected by the oxidation of Mn^{II} to Mn^{III}. Spectra for $x \leq 0.25$ cannot be fitted using only the same Fe^{III} doublet used for the fit of the spectra recorded in the plateau of the second region. Best fit is only obtained using one more Fe^{III} doublet with higher quadrupole splitting of 1.52 mms^{-1} indicating that the Mössbauer probe (Fe) is also sensitive to the oxidation occurring in Mn sites (Fig. 4).

Fig. 5 Galvanostatic curves for TiSnSb cell cycled at C/5 (1 Li/5 h) rate between 1.5 and 0. V
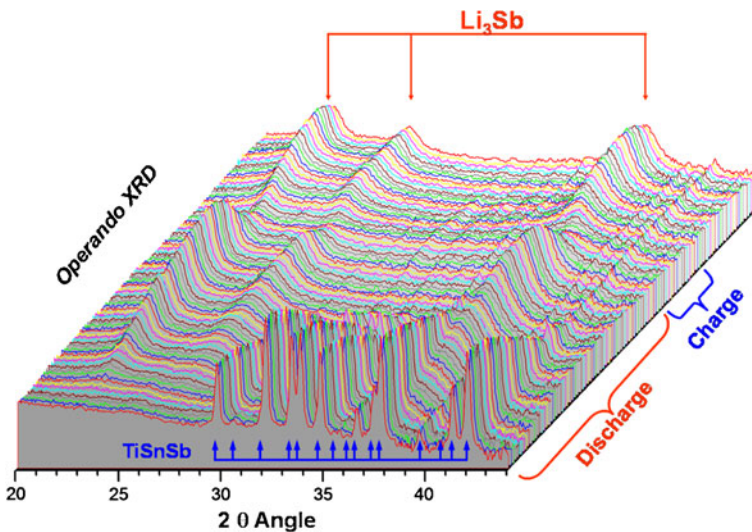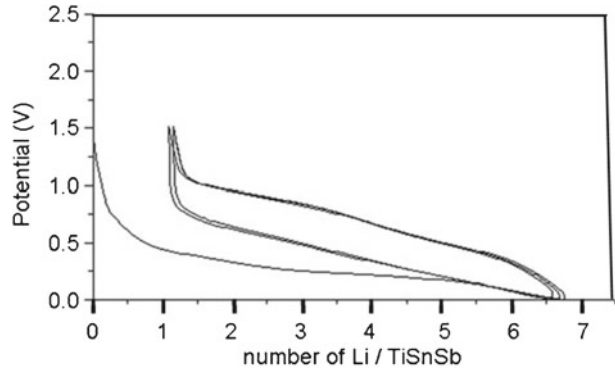

Fig. 6 *Operando* XRPD patterns of TiSnSb/Li cell in the 20–44° 2θ region (λ CuK$_\alpha$ 1.5418 Å)

The ability for this material to be used as positive electrode materials for power Li-ion batteries is now in progress.

4 TiSnSb as negative electrode

TiSnSb could be a new efficient negative electrode for Li-ion batteries. It can reversibly take up more than 5 Li per formula unit (Fig. 5) leading to reversible capacities of about 540 Ah/kg with a very good cycleability. The electrochemical mechanism has been studied from *operando* XRPD and ^{119}Sn TMS measurements [7]. The XRPD patterns (Fig. 6) show that the disappearance of the TiSnSb peaks is associated to the growth of very broad peaks which can be attributed to the cubic β Li$_3$Sb. Upon subsequent cycles the growth of Li$_3$Sb during discharge and its disappearance during charge is observed. This is indicative of a conversion reaction
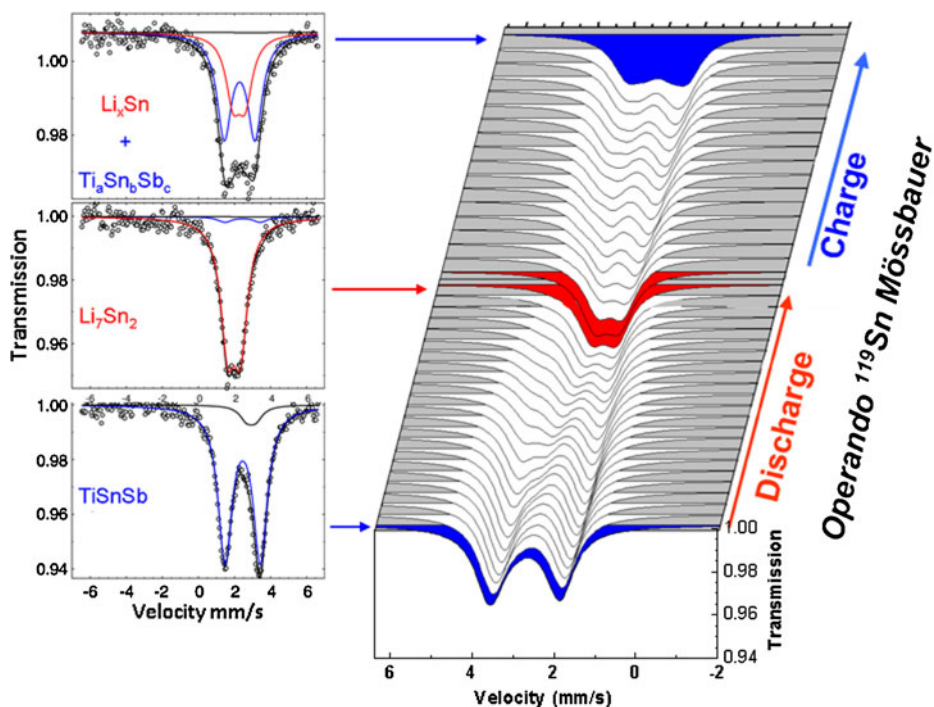
Fig. 7 *Operando* [119]Sn TMS spectra collected during the discharge/charge of TiSnSb/Li cell. The fitted spectra are relative to the pristine material (TiSnSb), the end of the 1st discharge (Li_7Sn_2) and the end of the 1st charge ($Li_xSn + Ti_aSn_bSb_c$)

process of TiSnSb into Li_3Sb and Ti nano-particles not visible by XRPD. At this point of the study, no information about tin reactivity has been obtained since no known Li-Sn intermetallic phase has been evidenced from the XRPD patterns (Fig. 6).

[119]Sn TMS was then used in the *operando* mode (Fig. 7) to follow the reactivity of Sn while cycling the TiSnSb powder. The charge discharge curves have been carried out in a rate of C/5 and Mössbauer spectra have been recorded each 85 min corresponding to the reaction of 0.28 Li. During the first discharge, the Mössbauer spectra start to exhibit significant changes only after the reaction of about 1.1 Li confirming that the observed electrochemical activity in this range is related to the reaction of Li with electrolyte and/or some surface phenomena (SEI). The changes consist of the appearance of a new Mössbauer absorption (doublet) having hyperfine parameters in the range of Li–Sn intermetallics. Even though this new doublet cannot be unequivocally attributed to one single Li–Sn intermetallic, the evolution of the average isomer shift ($<\delta>$) is a good indicator of the Li content in the formed phases [8].

At the beginning of the discharge, the high $<\delta>$ (2.25 mm/s) indicates the formation of Sn-rich intermetallics (typically in the range of LiSn and Li_7Sn_3). Further reaction of lithium induces a decrease of $<\delta>$ in agreement with Li-enrichment. At the end of the discharge, $<\delta>$ reaches 1.9 mm/s indicating the formation of

Fig. 8 Evolution of **a** the
average d of the Li_xSn phases,
b the relative amount of Li_xSn
and **c** of TiSnSb
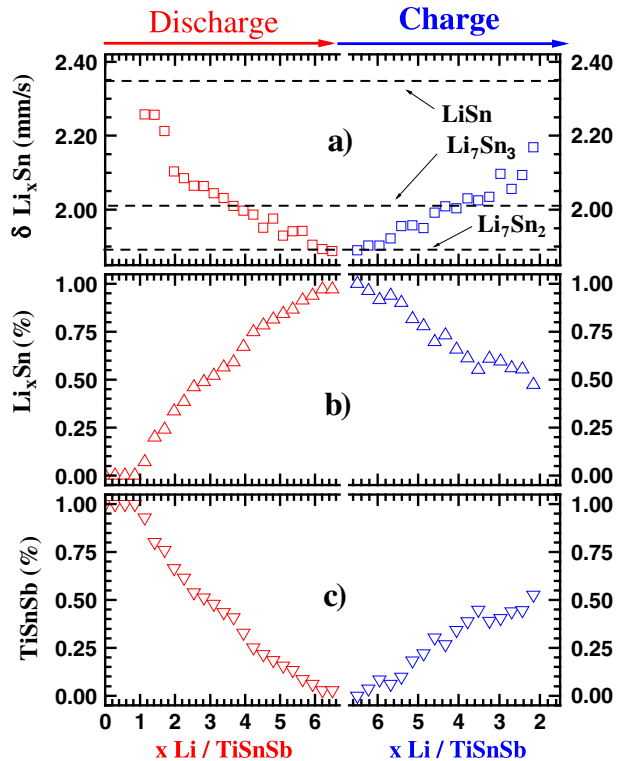
Li_7Sn_2. The evolutions of $<\delta>$ and relative amounts of TiSnSb and Li_xSn during
the discharge/charge processes are summarized in Fig. 8.

In the discharge process, a progressive conversion of TiSnSb into LiySb + LixSn
alloys is observed. At the end of the discharge Li_3Sb and Li_7Sn_2 are formed. During
the charge, a new Sn-based alloy is formed (likely a Sn-phase with Ti and/or Sb).
The role of Ti in the electrochemical mechanism has to be determined. The cycling
performances are currently evaluated and the preliminary test seems to show very
promising.

5 Conclusions

TMS is a powerful tool to characterize the local electronic structure around the
probed element in crystalline, glass, amorphous or nano-structured materials by
the determination of oxidation state, local coordination and bonding. It allows
identification of redox processes, characterisation of intermediate phases and makes
possible the study of reaction mechanisms thanks to a diversity of experimental
facilities.

In the field of Li-ion batteries, thanks to the design of specific electrochemical
cells, [119]Sn, and [57]Fe *operando* TMS have been combined with *operando* XRPD to
characterize new electrode materials. Gathering basic structural, textural, physical
information at the nano-scale provides a valuable scientific ground to better predict,

optimize and design performing electrodes components to the next generation of Li-ion batteries. Great insights into a better understanding of the electrochemical reaction from *operando* measurements have been obtained for promising new materials as $LiMn_{0.25}Fe_{0.75}PO_4$ for positive electrode or TiSnSb for negative electrode allowing the monitoring of complete cells. With the massive arrival of Sn-based composites or intermetallics joined with the advent of new Fe-based electrodes, TMS has a bright future. Such a spectroscopy could have a great impact on studying electrochemical and ageing mechanisms.

References

1. International Meeting on Lithium Batteries. IMLB 16, Jeju, Korea, 17–22 June 2012
2. Lippens, P.E., Jumas, J.-C.: Mössbauer spectroscopy investigation of batteries. Mössbauer Eff. Ref. Data J. **33**(2), 31–54 (2010)
3. Leriche, J.B., Hamelet, S., Shu, J., Morcrette, M., Masquelier, C., Ouvrard, G., Zerrouki, M., Soudan, P., Belin, S., Elkaïm, E., Baudelet, F.: An electrochemical cell for Operando study of lithium batteries using synchrotron radiation. J. Electrochem. Soc. **157**, A606–A610 (2010)
4. Pahdi, A.K., Nanjundaswamy, K.S., Goodenough, J.B.: Phospho-olivines as positive-electrode materials for rechargeable lithium batteries. J. Electrochem. Soc. **144**, 1188–1194 (1997)
5. Perea, A., Sougrati, M.T., Ionica-Bousquet, C.M., Fraisse, B., Tessier, C., Aldon, L., Jumas, J.-C.: Operando ^{57}Fe Mössbauer and XRD investigation of $Li_xMn_yFe_{1-y}PO_4/C$ composites (y = 0; 0.25). RSC Advances **2**, 2080–2086 (2012)
6. Perea, A., Sougrati, M.T., Ionica-Bousquet, C.M., Fraisse, B., Tessier, C., Aldon, L., Jumas, J.-C.: Operando ^{57}Fe Mössbauer and XRD investigation of $Li_xMn_yFe_{1-y}PO_4/C$ composites (y = 0.50; 0.75). RSC Advances **2**, 9517–9524 (2012)
7. Sougrati, M.T., Fullenwarth, J., Debenedetti, A., Fraisse, B., Jumas, J.-C., Monconduit, L.: TiSnSb a new efficient negative electrode for Li-ion batteries: mechanism investigations by operando-XRD and Mössbauer techniques. J. Mater. Chem. **21**, 10069–10076 (2011)
8. Robert, F., Lippens, P.-E., Olivier-Fourcade, J., Jumas, J.-C., Gillot, F., Morcrette, M., Tarascon, J.-M.: Mössbauer spectra as a fingerprint in tin-lithium compounds: Applications to Li-ion batteries. J. Solid State Chem. **180**, 339–348 (2007)